Rotary dynamics of solitons in radially periodic optical lattices

Keya Zhou (周可雅), Zhongyi Guo (郭忠义), and Shutian Liu (刘树田)*

Department of Physics, Harbin Institute of Technology, Harbin 150001, China

**E-mail: stliu@hit.edu.cn*

Received January 4, 2010

We investigate the dynamics of strongly localized solitons trapped in remote troughs of radially periodic lattices with Kerr-type self-focusing nonlinearity. The rotary motion of solitons is found to be more stable for larger nonlinear wavenumbers, lower rotating velocity, and shorter radius of the trapping troughs. When the lattice is shrunk or expanded upon propagation, the solitons can be trapped in the original trough and move outward or inward, with their rotating linear velocity inversely proportional to the radius of the trapping troughs.

OCIS codes: 190.0190, 190.4420, 190.6135.

doi: 10.3788/COL20100808.0791.

Solitons in nonlinear systems play a crucial role in many branches of nonlinear science, such as biology, solid state physics, Bose-Einstein condensates (BECs), and nonlinear optics[1−6]. In Kerr medium with a purely cubic nonlinear response, solitons formally exist, but in two- and three-dimensional (2D and 3D) cases, they are unstable against the spatiotemporal collapse induced by the combined effect of nonlinearity and diffraction (anomalous dispersion)[6]. One way to prevent collapse is to change the nonlinearity by considering media with quadratic (second-harmonic generating) nonlinearity or saturable nonlinearity. Another way is to introduce transverse modulation of potentials (optical lattices). In recent years, many interests have been directed to the latter case, and many properties of solitons that cannot be observed in bulk uniform nonlinear media have been discovered in transverse modulated media.

In the 2D domain, solitons have been investigated in harmonic lattices[7,8], hexagon lattices[9], axis-symmetric lattices[10−16], and other kinds of lattices[17−19]. Recently, axis-symmetric lattices have been the focus of attention, where solitons are trapped either at the center or in the remote troughs of the lattices. Different forms of solitons have been examined, such as fundamental solitons[10−12], dipole solitons[13], ring solitons, and necklace solitons[14]. An interesting phenomenon takes place in 2D Bessel lattices or radially periodic lattices. When fundamental solitons are probed into remote troughs, they take a rotary motion[10−12,15]. However, recent achievements in this field usually employ a fundamental soliton as the probe beam, which is not formally the exact solution of solitons trapped in remote troughs. Solitons that are trapped in remote troughs are determined by the local distribution of the refractive index and have different profiles from fundamental solitons. Their corresponding rotary dynamics has never been reported before.

In this letter, we begin our research with the 2D Gross-Pitaevskii equation (GPE)[15] with radially periodic potential. The profiles of solitons trapped in remote troughs of stationary lattices are obtained by Fourier iteration method[8]. Using the solved soliton profiles as input signals, their propagation dynamics are numerically simulated by the split-step Fourier transformation method (SSFTM). In stationary lattices, the rotating motion of a soliton is affected by the potential strength, nonlinear wavenumber, rotating velocity, and radius of the troughs. In particular, we also investigate the rotary motion of a soliton in dynamic lattices, which are shrunk or expanded upon propagation. In our simulation, we use a rather stable soliton profile as input signal and find that solitons are trapped in the original troughs and rotate around the axis in a spiral motion upon propagation. The rotating linear velocity is inversely proportional to the radius of the troughs, which is determined by the two conserved quantities of the GPE.

The model follows standard GPE in its normalized form[15]

$$\mathrm{i}\frac{\partial u}{\partial t}+\left(\frac{\partial^2}{\partial x^2}+\frac{\partial^2}{\partial y^2}\right)u+V(x,y)u+|u|^2u=0, \quad (1)$$

written for the wave function u in Cartesian coordinates (x,y). The equation can describe the evolution of matter-wave solitons created in BECs with respect to time, and $V(x,y)$ is the corresponding optical lattice potential. The dimensionless variables are chosen such that u is measured in units of the recoil energy $E_\mathrm{r}=\hbar^2k^2/2m$, where $k=\pi/d$, and d is a constant representing the scale of the lattices. The temporal coordinate t and spatial coordinates (x,y) are measured in units of $E_\mathrm{r}/\hbar$ and d/π, respectively. In our simulation, we consider periodic potential in the axial direction as

$$V(r)=\varepsilon\cos(2\pi r/T), \quad (2)$$

where ε is the modulation depth of the optical lattice potential, and $T=2\pi$ is the dimensionless period along the radial direction. The solitons trapped in the lattices can be written as $u(x,y,t)=U(x,y)\mathrm{e}^{\mathrm{i}\mu t}$, where μ is the nonlinear wavenumber of the solitons and $U(x,y)$ denotes the soliton profile. We use the Fourier iteration scheme used in Ref. [6], choose a Gaussian-like initial condition, and let the maximum of the trial function centered at the center of n_r be the lattice trough at points $(n_\mathrm{r}T,0)$.

After iteration, the profiles of the solitons can be found for given nonlinear wavenumbers that are trapped in the chosen troughs.

Equation (1) conserves two quantities, the power

$$P(\mu) = \int_{-\infty}^{+\infty} \int_{-\infty}^{+\infty} |U|^2 \mathrm{d}x\mathrm{d}y \tag{3}$$

and the angular momentum

$$\boldsymbol{L} = \frac{1}{2\mathrm{i}} \iint [(x\boldsymbol{i} + y\boldsymbol{j}) \times (U^* \nabla U - U \nabla U^*)] \, \mathrm{d}x\mathrm{d}y. \tag{4}$$

In what follows, we show that the above two conservative quantities are important for the rotary motion of solitons in radially periodic lattices, especially in dynamic lattices that are to be introduced in the following.

Without loss of validity and generality, we set $k = 2$ and find solitons that are trapped in the 5th trough of the lattice with different modulation depths. The corresponding lattice profile is shown in Fig. 1(a), with radial period $T = 2\pi/k = \pi$. The dependence of soliton power on the nonlinear wavenumber is depicted in Fig. 1(b) for $\varepsilon = 1$, 2, and 3, respectively. Two typical soliton profiles are shown in Figs. 1(c) and (d) with $\mu = 0.6$ and 3, as marked by circles in Fig. 1(b). Similar solitons that are trapped in the center and in remote troughs exist when μ is larger than a minimum value, which is larger for a deeper modulation of the potential (larger ε) as shown in Fig. 1(b). When μ is smaller, the corresponding solitons spread along the trough at first, and then into the nearby troughs, as shown in Fig. 1(c) as an example. When $\mu >> \varepsilon$, the solitons are strongly confined in the trough and slightly perturbed by the local refractive index potential, as seen in Fig. 1(d). Their power increases asymptotically to 11.7, which is constant in a bulk medium with Kerr-type nonlinearity[2].

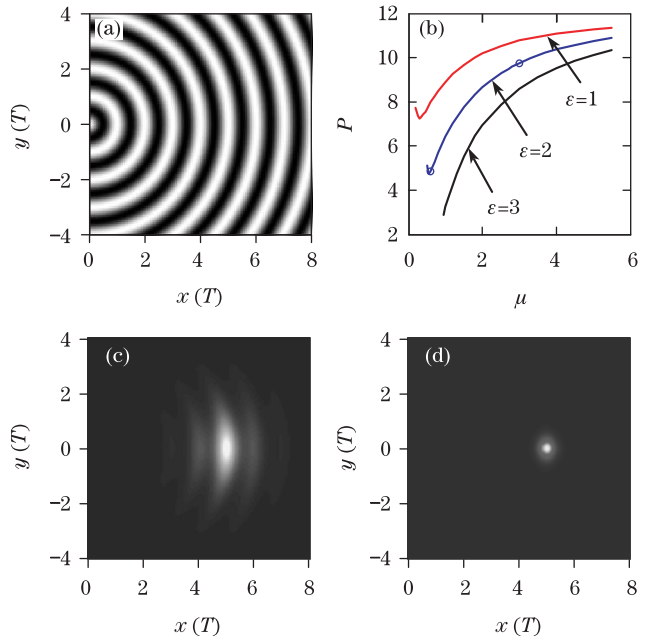

Fig. 1. (a) Radially periodic lattice with $T = \pi$; (b) soliton power P versus nonlinear wavenumber μ for solitons trapped in the 5th trough of a radially periodic lattice with $\varepsilon = 1$, 2, and 3; profile of solitons with nonlinear wavenumbers (c) $\mu = 0.6$ and (d) $\mu = 3$, respectively, trapped in the 5th trough of a radially periodic lattice with $\varepsilon = 2$.

The linear stability of solitons is determined by the well-known Vakhitov-Kolokolov (VK) criterion. Figure 1(b) shows that $\mathrm{d}P/\mathrm{d}\mu > 0$ is satisfied in most of the existence region for a small ε and in the entire existence region for a large ε. We also simulate the propagation of solitons perturbed by random noise using the SSFTM method and find that solitons are stable against linear perturbations, thereby proving the validity of the VK criterion.

A notable feature of axis-symmetric lattices is the rotation of solitons around certain lattice troughs[10−12,15]. To investigate this, we use the following expression

$$U_0(x, y) = U(x, y) \exp(\mathrm{i}vy), \tag{5}$$

where $U(x, y)$ is the soliton profile solved by the Fourier iteration method, and v is the initial velocity given to the soliton, as initial condition. The propagation of the beam is simulated using the SSFTM method. We define the percentage of soliton power that falls in the trapping trough by

$$\eta = \frac{P_{n_\mathrm{r}}}{P} = \frac{\int_{(n_\mathrm{r}-1/2)T}^{(n_\mathrm{r}+1/2)T} |U(x,y)|^2 \mathrm{d}x\mathrm{d}y}{\int_{-\infty}^{+\infty} |U(x,y)|^2 \mathrm{d}x\mathrm{d}y}. \tag{6}$$

The solitons become more confined in the trapping trough as μ increases, and other parameters are set stationary. The percentage of energy trapped in the original trough versus propagation distance is shown in Fig. 2(a) for different nonlinear wavenumbers. The solitons can travel around the lattice troughs with nearly no loss of energy when the nonlinear wavenumber is larger than 1.2. With μ decreasing, most of the energy radiates to other troughs when the solitons circulate around the trough. We also investigate the propagation of the solitons around troughs with different velocities. We find that higher velocities may cause some of the energy to tunnel into outer troughs, and the corresponding rotary motion is rather more unstable, as shown in Fig. 2(b). When driven by the same linear velocity, the solitons trapped in the second trough radiate most of their energy when $t > 30$, as shown in Fig. 2(c). Meanwhile, those solitons trapped in the 4th trough retain more than 98% of their energy as long as $t = 100$. Thus, soliton rotary motion in stationary lattices is more stable for larger nonlinear wavenumbers, lower initial linear velocities, and shorter distances away from the center of the lattices.

To further investigate the guiding properties of radially periodic lattices, we consider the soliton with nonlinear wavenumber $\mu = 3$ and trapped in the 5th trough; we let the optical lattice potential vary with time in a linear motion as

$$V(r, t) = \varepsilon \cos(kr + \alpha t). \tag{7}$$

The lattices shrink or expand for different signs of α. In Figs. 3(a) and (b), we demonstrate the track of the soliton in the transverse plane for $\alpha = \pm 0.1\pi$. The pictures are taken in a sequence of snapshots with steps

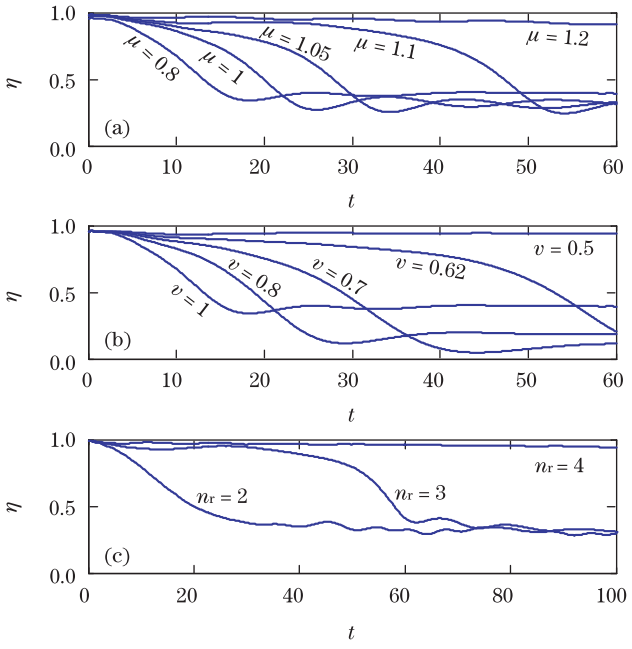

Fig. 2. (a) Percentage of energy trapped in the original trough η versus time for different μ values, the other parameters are $n_{\rm r} = 5$, $\varepsilon = 2$, and $v = 1$; (b) percentage of energy trapped in the original trough versus time for different velocities, the other parameters are $n_{\rm r} = 5$, $\varepsilon = 2$, and $\mu = 0.8$; (c) percentage of energy trapped in different troughs versus time, the other parameters are $\varepsilon = 2$, $v = 1$, and $\mu = 1.4$.

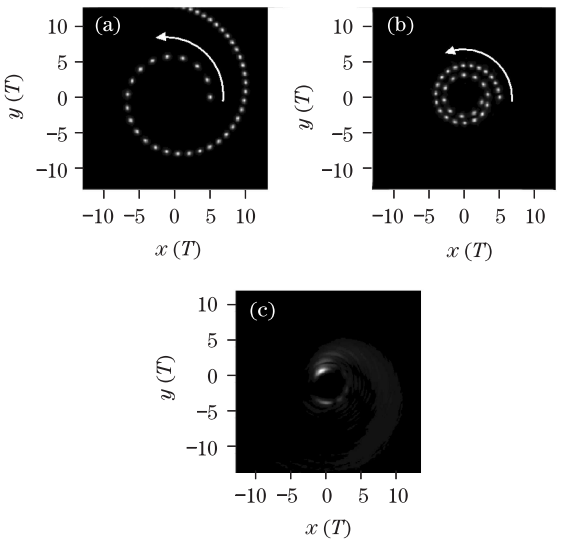

Fig. 3. (a) Soliton propagation for $\alpha = +0.1\pi$, $v = 1$, and $\mu = 3$, illustrated by a sequence of snapshots with $\mathrm{d}t = 4$; (b) soliton propagation for $\alpha = -0.1\pi, v = 1, \mu = 3$, illustrated by a sequence of snapshots with $\mathrm{d}t = 1.6$; (c) soliton profile after traveling along the propagating direction at $t = 160$; the parameters are the same as those in (b). White arrows in (a) and (b) mark the rotary direction of the solitons.

$\mathrm{d}t = 4$ and 1.6. The solitons take a spiral motion. Their linear velocity also changes while propagating. It decreases when the solitons are moving outward but increases when they are moving inward, corresponding to different signs of α. We find that the change in soliton rotating linear velocity can be interpreted by the admission of GPE of the conserved angular momentum $\boldsymbol{L}$ as shown in Eq. (4).

Assuming that the soliton is far from the lattice center and is highly confined in local troughs, we can use the following Gaussian ansatz for a soliton trapped in the point $(n_{\rm r}T, 0)$:

$$U(x,y) = A\exp\left[-\frac{(x-r_0)^2+y^2}{\omega_0^2}\right]\mathrm{e}^{\mathrm{j}vy}, \tag{8}$$

where $r_0 = n_{\rm r}T$, and A and ω_0 are the two constants that determine the amplitude and size of the soliton, respectively. We substitute the above expression into Eq. (4) and obtain

$$\begin{aligned} U^*\nabla U =& A^2\left[-\frac{2x}{\omega_0^2}\boldsymbol{i} + \left(-\frac{2y}{\omega_0^2} + \mathrm{i}v\right)\boldsymbol{j}\right] \\ &\times \exp\left[-\frac{2(x-r_0)^2+2y^2}{\omega_0^2}\right]. \end{aligned} \tag{9}$$

Then the conserved angular momentum only has component along the temporal coordinate, and it reads

$$L_{\rm t} = \iint xv\exp\left[-\frac{2(x-r_0)^2+2y^2}{\omega_0^2}\right]\mathrm{d}x\mathrm{d}y. \tag{10}$$

The right hand side of Eq. (10) is reduced to $L_{\rm t} \approx r_0 vP$ under the approximation that $r_0 >> T$ and ω_0. Notably, the above conserved angular momentum is an inherent attribute of the GPE and is different from the angular momentum of solitons. P and $\boldsymbol{L}$ are the two conserved quantities of GPE, so the above expression shows that the linear velocity of solitons is inversely proportional to the radius of the trapping troughs: solitons move outward when the lattice is tuned, and they expand upon propagation ($\alpha > 0$), so their linear velocity has to decrease in order to conserve the angular momentum. When $\alpha < 0$, the solitons move inward, and their velocity increases.

When the solitons move too close to the center, their linear velocity becomes so high that they cannot maintain their shapes and gradually radiate some of their energy. A typical example is shown in Fig. 3(c), wherein the soliton eventually disappears after propagating as far as $t = 160$. This result is similar with the case shown in Fig. 2(b) for higher linear velocities. The only difference is that the linear velocity increases in the dynamic lattices rather than in an initially imposed condition.

In conclusion, we investigate the rotary dynamics of matter-wave solitons in BECs with a radially periodic optical lattice potential. The profiles of the solitons trapped in certain troughs are found. Both stationary and dynamic lattices are considered. When set in rotary motion, the solitons may be trapped in the troughs or radiate some of their energy to other troughs. Larger nonlinear wavenumbers or smaller velocities can help stabilize the rotation. Further, the solitons are more likely to be trapped in the outer troughs of radially periodic lattices. When the potential expands or shrinks with time, the solitons are trapped in the original trough and take a spiral motion, with their linear velocity decreasing or increasing at the same time, which is inversely proportional to the radius of the trapping troughs. Our findings enrich current knowledge on the rotary motion of solitons in radially periodic lattices and may pave the way for the future applications of spatial solitons in 2D regimes in both nonlinear optics and BECs.

This work was supported by the National Natural Science Foundation of China (Nos. 10674038 and 10974039) and the National Basic Research Program of China (No. 2006CB302901).

References

1. Y. S. Kivshar and G. P. Agrawal, *Optical Solitons: From Fibers to Photonic Crystals* (Academic Press, San Diego, 2003).
2. M. H. Li, Chin. Phys. B **16,** 3187 (2007).
3. N. Ding and Q. Guo, Chin. Phys. B **18,** 4298 (2009).
4. J. Zhou, X. Meng, C. Ren, Y. Gao, and M. Chen, Acta Opt. Sin. (in Chinese) **29,** 2270 (2009).
5. Y. Zhang, C. Hou, and X. Sun, Chinese J. Lasers (in Chinese) **35,** 694 (2008).
6. Y. Silberberg, Opt. Lett. **15,** 1282 (1990).
7. J. W. Fleischer, M. Segev, N. K. Efremidis, and D. N. Christodoulides, Nature **422,** 147 (2003).
8. Z. H. Musslimani and J. K. Yang, J. Opt. Soc. Am. B **21,** 973 (2004).
9. V. S. Shchesnovich, A. S. Desyatnikov, and Y. S. Kivshar, Opt. Express **16,** 14076 (2008).
10. Y. V. Kartashov, V. A. Vysloukh, and L. Torner, Phys. Rev. Lett. **93,** 093904 (2004).
11. X. S. Wang, Z. G. Chen, and P. G. Kevrekidis, Phys. Rev. Lett. **96,** 083904 (2006).
12. Y. J. He, B. A. Malomed, and H. Z. Wang, Phys. Rev. A **76,** 053601 (2007).
13. Y. V. Kartashov, A. A. Egorov, V. V. Vysloukh, and L. Torner, J. Opt. B: Quantum Semiclass. Opt. **6,** 444 (2004).
14. L. W. Dong, H. Wang, W. D. Zhou, X. Y. Yang, X. Lv, and H. Y. Chen, Opt. Express **16,** 5649 (2008).
15. B. B. Baizakov, B. A. Malomed, and M. Salerno, Phys. Rev. E **74,** 066615 (2006).
16. J. Scheuer and B. Malomed, Phys. Rev. A **75,** 063805 (2007).
17. M. J. Ablowitz, B. Ilan, E. Schonbrum, and R. Piestun, Phys. Rev. E **74,** 035601 (2006).
18. A. Ruelas, S. Lopez-Aguayo, and J. C. Gutiérrez-Vega, Opt. Lett. **33,** 2785 (2008).
19. L. Moretti and V. Mocella, Opt. Express **15,** 15314 (2007).